Heat Transfer Applications of Metallic Femtosecond Laser Processed Surfaces: Pool Boiling and Self-Propelled Droplets

Corey Kruse, Anton Hassebrook, Troy Anderson, Chris Wilson, Craig Zuhlke, Dennis Alexander, George Gogos, and Sidy Ndao
University of Nebraska – Lincoln http://nmrl.unl.edu

Motivation

- Femtosecond Laser Surface Processing (FLSP) has the ability to functionalize metallic surfaces with self-organized micro/nanostructures capable of the following:

Heat Transfer Application

- Increase temperature range of efficient nucleate boiling regime
- Increase Critical Heat Flux
- Increase effective Heat Transfer Coefficient
- Take advantage of Leidenfrost State
- Using an asymmetric angled microstructures, liquid droplets can be propelled across a surface

Traditional Boiling Curve

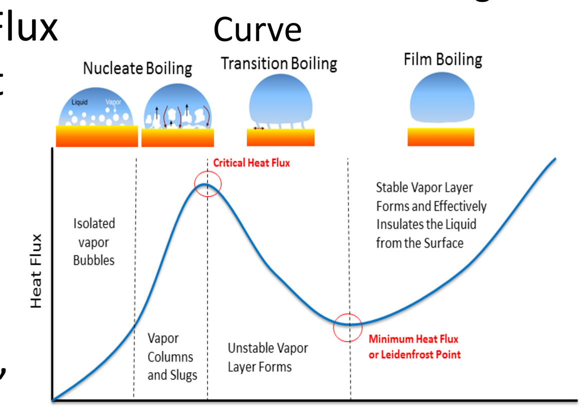

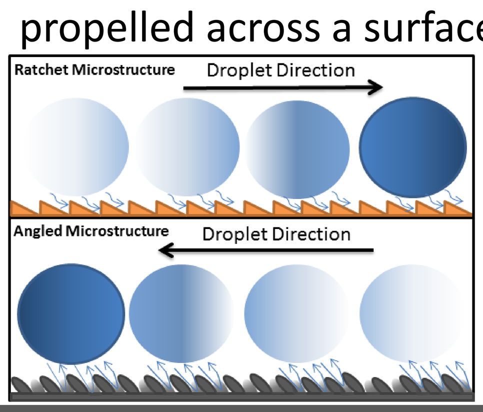

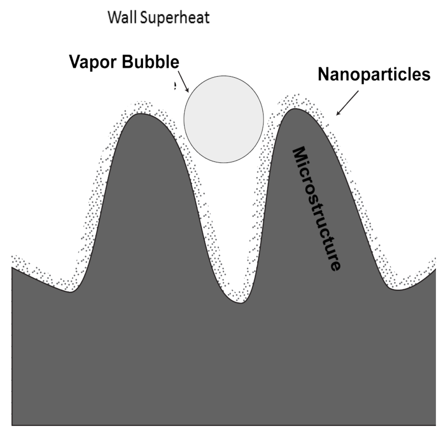

Pool Boiling Heat Transfer Enhancement

Experimental Setup

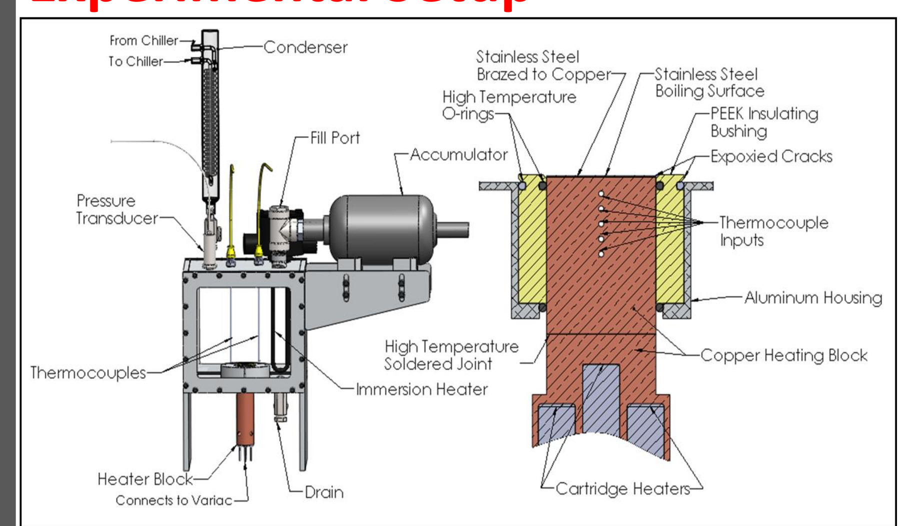

- For the BSG and ASG mounds, increases in critical heat flux was a result of increased capillary wicking due to densely packed microstructures
- The increase in heat transfer coefficient was directly related to an increase in surface area ratio and structure height
- Low temperature heat transfer enhancement is due to the increase in potential nucleation site density and increased nucleation efficiency.
- The NC-Pyramid Structures results in a relatively thick nanoparticle layer that covers a core microstructure.
- This nanoparticle layer was shown to insulate the surface and decrease the heat transfer coefficient
- The nanoparticle layer does result in a porous layer that promotes an increase in critical heat flux
- Only the LIPSS surface and the surface with a partially removed nanoparticle layer resulted in an increase in heat transfer coefficient
- When the nanoparticle layer is partially removed, the effective thermal resistance is lowered and local hot spots can form resulting in easily activated nucleation sites and a higher heat transfer coefficient.

BSG and ASG Mounds

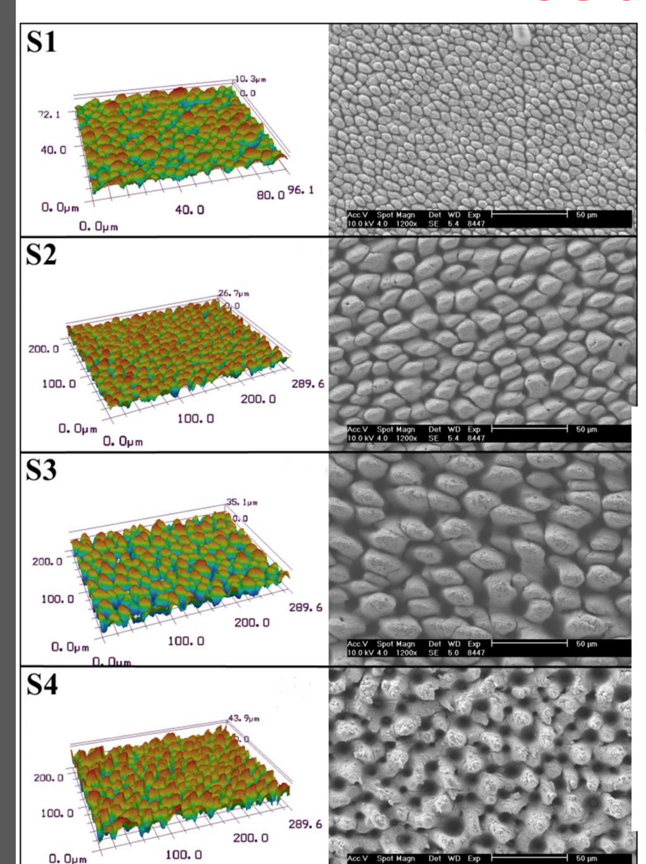

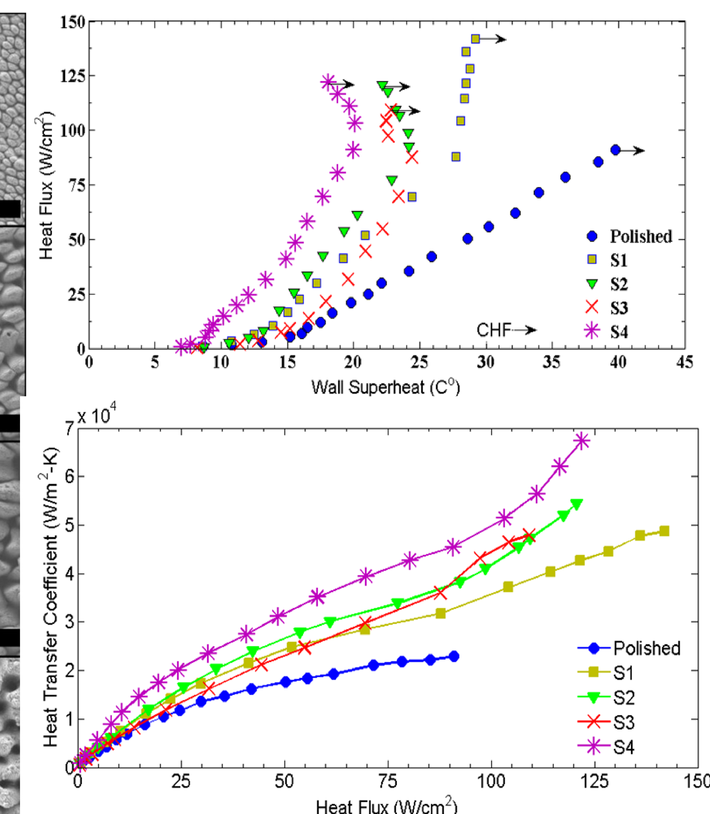

- S1-S3 had an increasing microstructure peak-to-valley height, surface roughness, and microstructure separation but had a nearly constant surface area ratio
- S4 resulted in a much higher surface area ratio and the tallest peak-to-valley height, but a smaller separation than S3

Sample	Fluence (J/cm²)	Number of Shots	Peak to Valley Height (μm)	Surface Roughness (μm)	Surface Area Ratio	Separation (μm)	CHF (W/cm²)	Superheat (C°)
Polished	--	--	--	0.22	1.09	--		
S1	0.7	840	7.1	1.4	3.85	6.0	142	29.2
S2	1.4	840	22.3	4.6	3.79	15.9	121	22.2
S3	2.1	840	31.3	7.8	3.82	26.1	110	22.8
S4	4.1	230	35.8	7.4	4.7	20.1	122	18.1

NC-Pyramids: Nanoparticle Effect

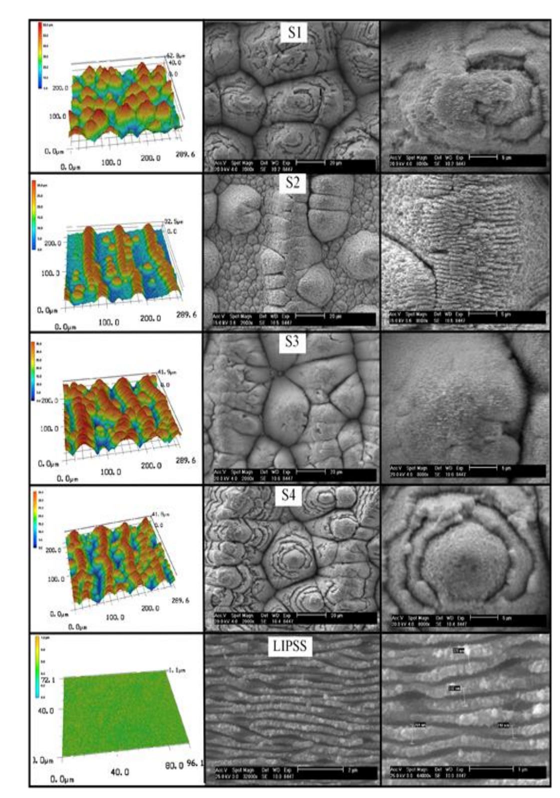

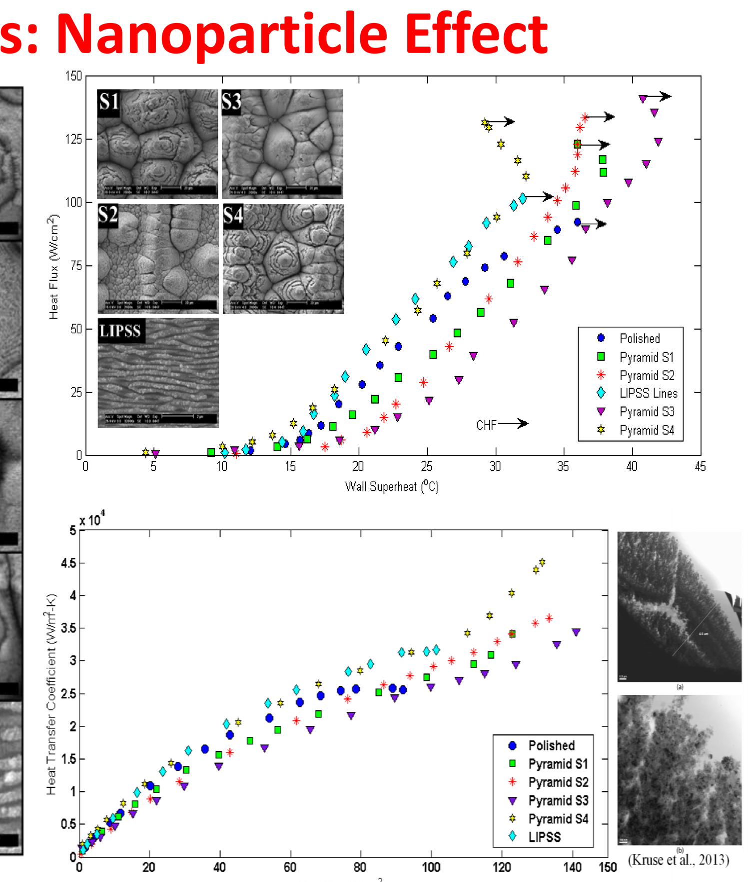

- S1 and S2 are NC-Pyramid Structures with varying Fluence and Shots
- S3 and S4 are identical structures but S4 endured a 1 hour ultrasonic bath to remove part of the nanoparticle layer
- The LIPSS sample has only nanosized features and is not superhydrophilic and does not display any wicking

Sample	Peak Fluence (J/cm²)	Pulse Count	Peak-to-Valley Height (μm)	Surface Roughness (μm)	Surface Area Ratio	Contact Angle	CHF (W/cm²)	Superheat (C°)
Polished	--	--	--	0.22	1.09	80	92	36
Pyramid S1	0.294	17034	47.2	11.8	3.63	0	122.6	36
Pyramid S2	0.389	2997	25.8	8.2	2.72	0	133.3	36.5
Pyramid S3	0.368	6518	35.5	9.58	3.03	0	141	40.8
Pyramid S4	0.368	6518	33.5	9.19	3.16	0	131.5	29.2
LIPSS Lines	0.385	86	0.89	0.113	1.63	65	101.3	32

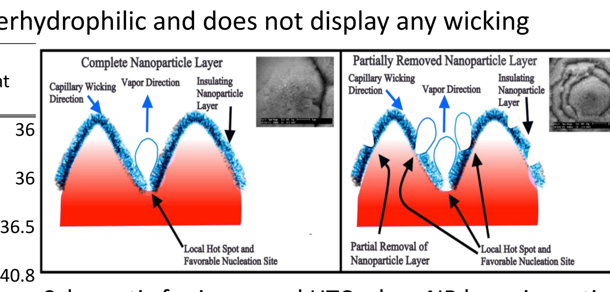

Schematic for increased HTC when NP layer is partially removed

Nano and Microstructure Fabrication

Machining Process

- Spectra-Physics Spitfire Laser
  - 50 fs
  - 1 mJ maximum pulse energy
  - 1 kHz repetition rate
  - 800 nm center wavelength

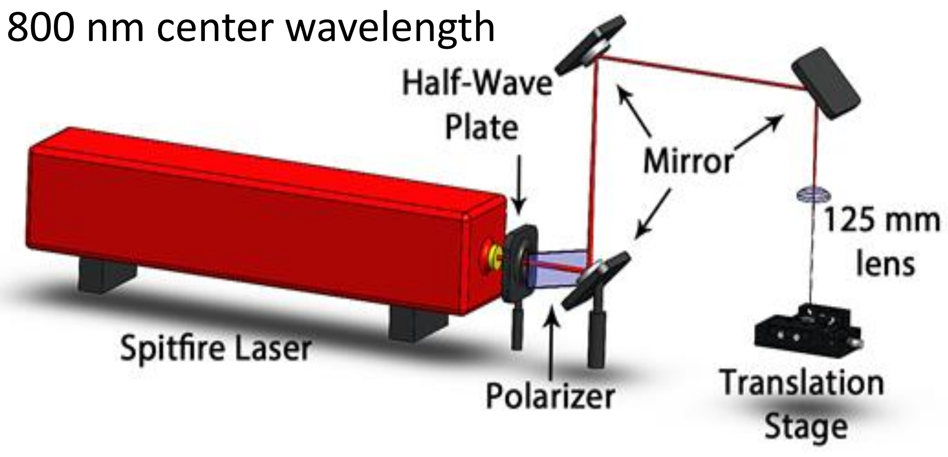

- Raster Path On Sample

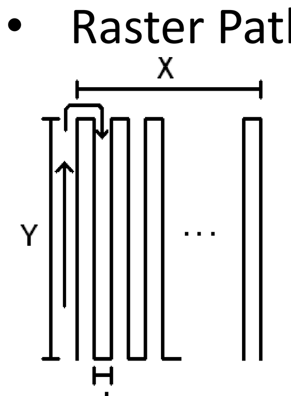

- Nanoparticle redeposition and surface fluid flow create micro and nano-structures.

- Range of Structures
  - A variety of structures can be created through the control of laser fluence and number of incident laser pulses
- Structures of interests for heat transfer include:
  - Pyramids
  - BSG-Mounds
  - ASG-Mounds

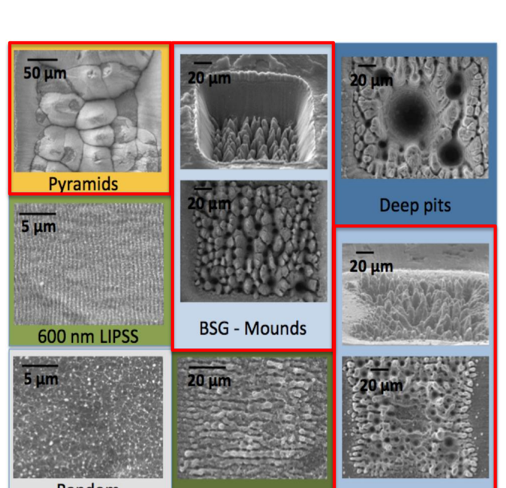

Self-Propelled Leidenfrost Drops

Experimental Setup

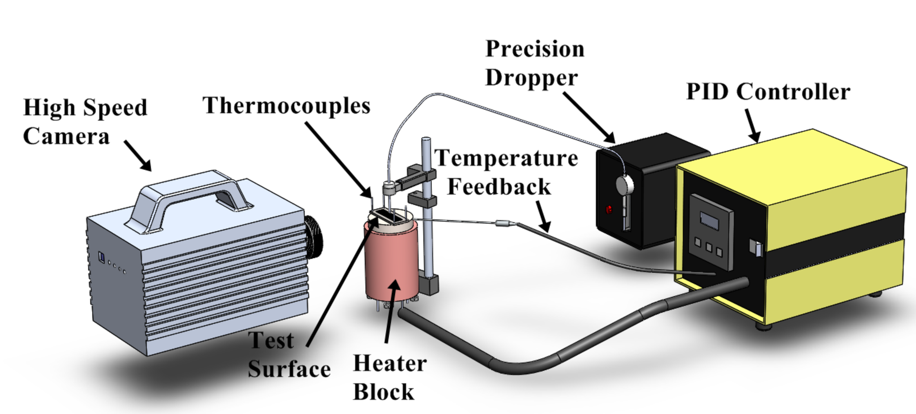

- Test surface is heated with precision controlled heating block
- 10.5 μL droplets are dispensed from a precision dropper
- Droplet motion is recorded with a high speed camera at 250 fps.

Angled Microstructure Fabrication

- The laser beam is focused at an incident angle which creates an angled (fish scale like) microstructure
- Structures were created with a 45 and 10 degree incident angle

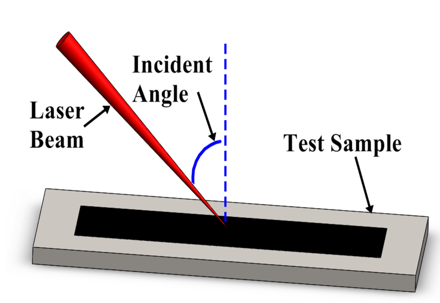

Structure Angle	Pulse Energy (μJ)	Number of Laser Shots	Spot Dia. (μm) (Parallel)	Spot Dia. (μm) (Perpendicular)	Peak-to-Valley Height (μm)	Structure Spacing (Parallel) (μm)	Structure Spacing (Perpendicular) (μm)
45	700	500	328	232	17	27	17
10	700	500	188	224	57	29	30

Surfaces

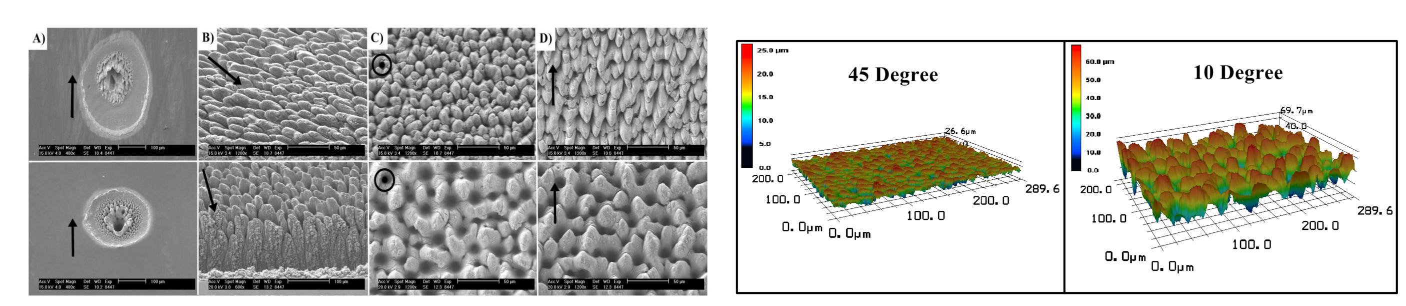

- Top: 45 degree surface, Bottom: 10 degree surface
- Surfaces were created with same processing power but resulted in different sizes due to the change in effect fluence and actual spot size

Data

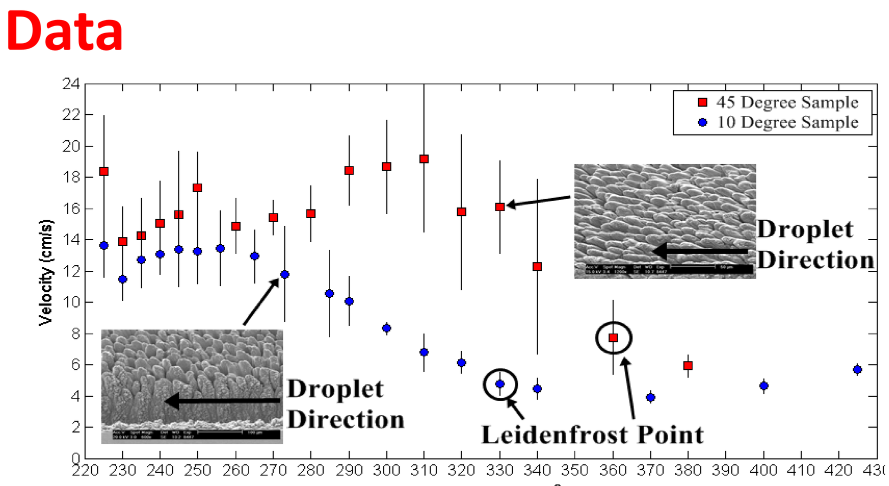

- Surface temperature was varied and droplet velocity was recorded at each step
- Droplets were consistently propelled in the opposite direction compared to conventional ratchet structures
- Two propulsion mechanisms are observed: Rocket like effect at temperatures below the Leidenfrost temperature and viscous drag mechanism above the Leidenfrost
- Rocket like effect results in higher velocities due to the intermittent contact which results in explosive propulsion
- Viscous drag mechanism results in a smooth propulsion force due to no intermittent contact

Mechanism for Alternate Droplet Direction

- Conventional ratchet surface is shown on top
- Due to the channels in the y direction, flowing vapor can escape in the y direction and drags the droplet in the x direction
- For angled microstructure the 3D nature prevents the vapor from escaping in the y direction and must be redirected resulting in an opposite droplet direction

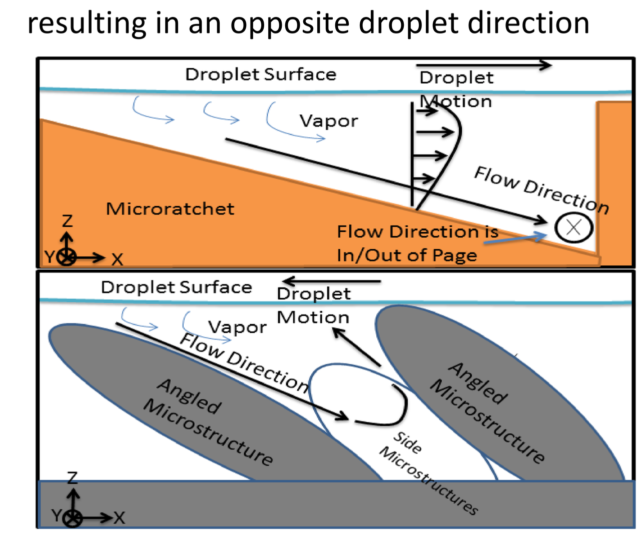

Acknowledgements

This work has been supported by a grant through the Nebraska Center for Energy Sciences Research (NCESR) with funds provided by Nebraska Public Power District (NPPD) to the University of Nebraska – Lincoln (UNL) No. 4200000844, a NASA EPSCoR Grant # -NNX13AB17A and by funds from the Department of Mechanical and Materials Engineering and the College of Engineering at UNL, awarded to SN.

nano & micro Systems Research Laboratory
University of Nebraska Lincoln
NEBRASKA CENTER FOR ENERGY SCIENCES RESEARCH